Bimetric universe with matter

Carlos Maldonado[*] and Fernando Méndez[†]

Universidad de Santiago de Chile, Facultad de Ciencia, Departamento de Física, Avenida Ecuador 3493, Estación Central Santiago, Chile 9170124

(Received 4 February 2021; accepted 21 April 2021; published 3 June 2021)

We analyze the early stage of evolution of a universe with two scale factors proposed in Falomir *et al.* [Phys. Rev. D **96**, 083534 (2017)]. when matter is present. The scale factors describe two causally disconnected patches of the universe interacting trough a nontrivial Poisson bracket structure in the momentum sector characterized by one parameter κ. We studied two scenarios in which one of the patches is always filled with relativistic matter while the other contains relativistic matter in one case, and nonrelativistic matter in the second case. By solving numerically the set of equations governing the dynamics, we found that the energy content of one sector *drains* to the other and from here it is possible to constrain the deformation parameter κ by supposing that the decay of the energy density happens, at most, at the Big Bang Nucleosynthesis temperature in order to return to the usual behavior of radiation. The relation with nonstandard cosmologies is also addressed.

DOI: 10.1103/PhysRevD.103.123505

I. INTRODUCTION

Our present description of the universe rests on the cosmological principle—the hypotheses of spatial homogeneity and isotropy at large scales—described by a Friedman-Lemaitre-Robertson-Walker (FLRW) metric [1,2]. Observations of rotational curves of galaxies [3,4] (for a review see [5,6]) as well as the observed accelerated cosmic expansion [7,8], made it necessary to complete the model with two extra hypotheses: the existence of dark matter and dark energy (cosmological constant term Λ), respectively. Thus, our present model of the universe, according to observations [9], contains 68.3% of dark energy, 26.8% of cold (nonrelativistic) dark matter, and 4.9% of baryonic matter.

On the other hand, possible traces of inhomogeneities[1] have been smoothed out during the exponentially accelerated period of expansion known as *inflation* [14,15], a new hypothesis which also solves the flatness and horizon problems, explains the origin of large-scale structures in the universe, and restores homogeneity inside the cosmological horizon.

In this regard, in a recent set of papers [16–18] a model for a universe with two metrics was considered. In such model, two regions (patches) causally disconnected after the inflation era, are described with metrics of FLRW type with different scale factors for each patch, and a sort of interaction was introduced through a deformation of the Poisson bracket structure in the space of fields. It was shown that, in absence of matter, this sort of interaction emulates the presence of cosmological constant on each patch.

Two comments are in order here. First, one should note that, in general, theories with two metrics develop ghost instabilities [19] since they contain a massive graviton (see for example [20]). However, for a class of massive gravity such inconsistencies can be avoided [21,22] even if the background metric is dynamic, as it was proved in [23,24]. The model we study in this work, on the other hand, introduces the interaction through a deformation of the algebra of canonical variables, and, then, the consistency problem might not be present. The complete analysis of the problem, in any case, goes beyond the scope of the present work and will be reported elsewhere in the future.

It should also be noted that the Poisson bracket structure deformation has been also previously considered [25–28], and, recently, in the context of closed strings on a flat background [29,30], which are the starting points for the recently proposed idea of *metaparticles* [31], that is, particles (as a world-line) defined in a doubled phase space with a nonstandard symplectic structure.[2] The implications for cosmology of this noncommutativity inspired from the string theory analysis have been discussed in [35].

In the present paper we extend the model in [16], in order to incorporate matter assuming that matter evolves independently on each sector and it can be modeled as a barotropic perfect fluid. We will show that this model

[*]carlos.maldonados@usach.cl
[†]fernando.mendez@usach.cl

[1]The possibility of formation of cosmic strings, monopoles, or domain walls can not be discarded from a theoretical point of view [10–13].

[2]For a general discussion on modular spacetime see [32–34].

can be understood as a sort of nonstandard cosmology (NSC) [36–42], for different values of the parameter controlling the Poisson's bracket deformation.

In order to do that, in the next section we will show the main features of the model with two metrics and the NSC scenario. Section III is devoted to the discussion of how to incorporate matter into the model. In Sec. IV two cases will be addressed: a) one patch filled with relativistic matter while the second one contains a nonrelativistic fluid and b) both patches containing relativistic matter. In the final section we present the conclusions and discuss possible extensions of the model.

II. THE TWO-METRIC UNIVERSE

The model discussed in [16] (see also [17,18]) describes two patches of the universe through scale factors $a(t)$ and $b(t)$, and a Hamiltonian

$$H = \frac{NG}{2}\left[\frac{\pi_a^2}{a} + \frac{1}{G^2}\left(ak_a - \frac{\Lambda_a}{3}a^3\right)\right] + \frac{NG}{2}\left[\frac{\pi_b^2}{b} + \frac{1}{G^2}\left(bk_b - \frac{\Lambda_b}{3}b^3\right)\right], \tag{1}$$

$$\equiv H_a + H_b, \tag{2}$$

where π_a, π_b are the conjugate momenta of a and b, respectively. Scale factors are chosen with canonical dimension -1, and then momenta have dimension $+1$.[3] N is an auxiliary field that guarantees the time reparametrization invariance. Patches a, b have spatial curvature k_a, k_b and cosmological constant Λ_a, Λ_b, respectively.

The Poisson bracket structure, on the other hand, is defined through the following relations:

$$\{a_\alpha, a_\beta\} = 0, \qquad \{a_\alpha, \pi_\beta\} = \delta_{\alpha\beta}, \qquad \{\pi_\alpha, \pi_\beta\} = \theta\epsilon_{\alpha\beta}, \tag{3}$$

with θ a constant parameter and index $\{\alpha,\beta\} \in \{a,b\}$. Scale factors notation is $a_a = a$, $a_b = b$. It is convenient to redefine the parameter θ as $\theta = \kappa G^{-1}$ with κ a dimensionless parameter.

Equations of motion derived from Hamiltonian (1) with Poisson brackets (3) are

$$\dot{a} = G\frac{\pi_a}{a}, \qquad \dot{b} = G\frac{\pi_b}{b}, \tag{4}$$

$$\dot{\pi}_a = G\frac{\pi_a^2}{2a^2} + \frac{1}{2G}(a^2\Lambda_a - k_a) + \kappa\frac{\pi_b}{b}, \tag{5}$$

$$\dot{\pi}_b = G\frac{\pi_b^2}{2b^2} + \frac{1}{2G}(b^2\Lambda_b - k_b) + \kappa\frac{\pi_a}{a}, \tag{6}$$

while the constraint $\dot{\pi}_N = 0$ reads

$$\frac{\pi_a^2}{a} + \frac{\pi_b^2}{b} + G^{-2}\left(ak_a + bk_b - \frac{\Lambda_a}{3}a^3 - \frac{\Lambda_b}{3}b^3\right) = 0. \tag{7}$$

Note that we have written the equations in the usual gauge $N = 1$ (equivalently, we have redefined the time variable $dt' = N(t)dt$).

Equations (4) to (7) can be recast as the following set of second order differential equations:

$$2a\ddot{a} + \dot{a}^2 = \Lambda_a a^2 - k_a + 2\kappa\dot{b}, \tag{8}$$

$$2b\ddot{b} + \dot{b}^2 = \Lambda_b b^2 - k_b - 2\kappa\dot{a}, \tag{9}$$

$$a\dot{a}^2 + b\dot{b}^2 = \frac{\Lambda_a}{3}a^3 - k_a a + \frac{\Lambda_b}{3}b^3 - k_b b. \tag{10}$$

The model presents several interesting properties as, for example, the existence of solutions containing both accelerated and decelerated periods or the presence of an inflationary epoch in a patch with a negligible cosmological constant (for example, for $\Lambda_a \ll \Lambda_b$). Note also that the equations are symmetric under the simultaneous change $a \to b$, $b \to a$, and $\kappa \to -\kappa$.

The effect of matter in the model, on the other hand, has not been explored and it is the main purpose of the present work to investigate this scenario. We will show that this two-metric model with matter has similar features compared with the nonstandard cosmologies (NSCs) scenarios.

Indeed, the study of the effects of different cosmological histories at early stages of the universe, such as matter domination ($H \propto T^{3/2}$) [38], kination domination ($H \propto T^6$) [43], or even a field with a general state of equation ($H \propto T^{3(\omega+1)/2}$) [40–42], where H is the Hubble parameter, is a very active field of research.

A particular scenario relevant to the present work considers the introduction of a field (ϕ) whose only effect is to modify the expansion rate of the universe, making it faster or slower (and also can decay into Standard Model particles). These kind of different cosmological histories are usually called nonstandard cosmologies (NSCs) and the only restriction for this new field is to decay before the epoch of Big Bang Nucleosynthesis (BBN), in order to not be in conflict with astrophysical measures [44,45].

For a general NSC model, the evolution equations read

$$\dot{\rho_{\rm SM}} + 4H\rho_{\rm SM} = \Gamma\rho_\phi \tag{11}$$

$$\dot{\rho_\phi} + 3(\omega+1)H\rho_\phi = -\Gamma\rho_\phi, \tag{12}$$

where $\rho_{\rm SM}$ is the energy density of the Standard Model (SM) content, ρ_ϕ is the energy density of the new field, ω is the constant for the barotropic fluid, Γ the decay constant for the ϕ field, and H is the Hubble parameter.

[3]The canonical dimensions of fields are chosen in this way just because of a matter of convenience.

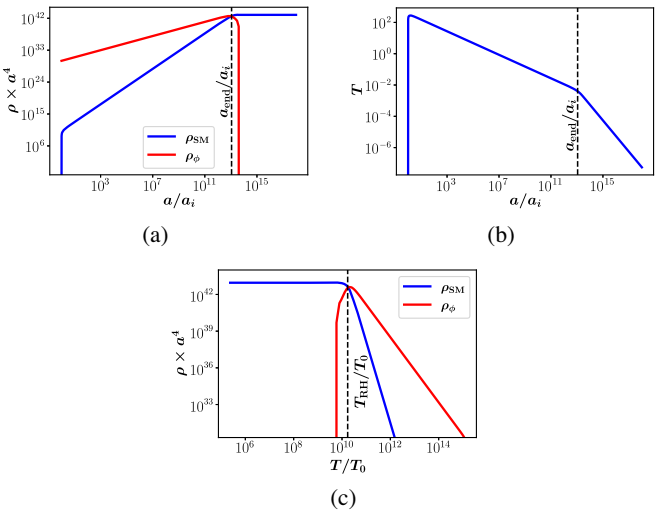

FIG. 1. Panel (a) shows the ϕ field acting like an inflaton. The SM sector starts to grow with the evolution of ϕ until $T_{\rm RH} = 4 \times 10^{-3}$ GeV is reached and ϕ decays. In panel (b) the temperature as a function of a/a_i is shown. The change of slope at $T_{\rm RH}$ is due to the decay of the ϕ field. Energy density as function of T is shown in (c), with $T_0 = 2.33 \times 10^{-13}$ GeV.

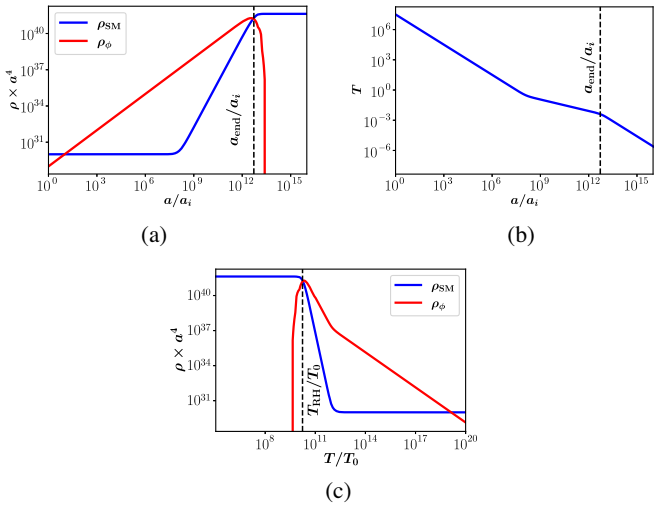

FIG. 2. Panel (a) shows the evolution of energy density of ϕ field and the SM bath for $\delta = 10^{-1}$. Γ is chosen so that ϕ decays at $T_{\rm RH} = 4 \times 10^{-3}$ GeV. Panel (b) exhibits the temperature as a function of a/a_i. The slope changes due to the effect of the ϕ field which is decaying. Panel (c) shows the relationship between the energy densities and the temperature, with $T_0 = 2.33 \times 10^{-13}$ GeV the current temperature.

The decay constant Γ can be expressed in terms of the reheating temperature $T_{\rm RH}$ (sometimes called $T_{\rm end}$ depending on the behavior of the ϕ field), by demanding

$$\Gamma = \frac{\pi}{3}\sqrt{\frac{g_\star}{10}}T_{\rm RH}^2, \tag{13}$$

that is, Γ is equal to the value of the Hubble parameter at the time when universe is dominated by radiation again. Here, g_* is the degrees of freedom of radiation that we will consider as a constant with value $g_\star \approx 10$, which corresponds to a temperature for $T_{\rm RH}$ (or $T_{\rm end}$) of $T = 4 \times 10^{-3}$ GeV. This value is imposed by the BBN epoch and corresponds to the lowest value of the temperature at which this new field must decay [46,47].

The ϕ field has interesting features. It acts like an inflaton when the initial energy density $\rho_{\rm SM}$ is zero and then generates a new epoch of reheating due to the decay term which transfers energy to the SM content until $T_{\rm RH}$ is reached [38,40]. At this temperature the ϕ field decays completely. This effect is shown in Fig. 1.

For a less restrictive scenario, one assumes a nonzero ratio between the energy density of ϕ and the energy density of the SM, at some initial scale factor a_i. That is, a nonzero value for the quantity

$$\delta = \left.\frac{\rho_\phi}{\rho_{\rm SM}}\right|_{a_i}.$$

In this case, this new field does not act like an inflaton anymore, but we can observe a similar behavior growing up the energy density for the SM content meanwhile the ϕ field is decaying until $T_{\rm end}$, which is the temperature when total decay occurs [42].

It is interesting to note that the two-metric model in absence of matter also shows an inflatonlike behavior [16], but there the interaction provided by the deformation of the Poisson bracket structure is responsible for such effect. We will show that for the matter case, it is possible to reproduce also the behavior shown in Fig. 2.

III. THE MATTER CONTENT

We are interested in the study of energy density evolution under the hypothesis that the evolution of matter in one patch is independent from the other and particularized to barotropic perfect fluids characterized by the pressure p and the energy density ρ.

Note that the lhs of (8) and (9) are proportional to the spatial component of the Einstein tensor. Indeed, for a FLRW metric with scale factor a and spatial curvature k_a (in the gauge $N = 1$) the Einstein tensor reads

$$G_{ij} = -g_{ij}(2a\ddot{a} + \dot{a}^2 + k_a), \qquad G_{00} = \frac{3}{a^2}(\dot{a}^2 + \kappa_a), \tag{14}$$

and then, under the hypothesis previously explained, we propose the following modification of the equations of motion in order to include matter effects:

$$2a\ddot{a} + \dot{a}^2 = \Lambda_a a^2 - k_a + 2\kappa\dot{b} - a^2 p_a, \tag{15}$$

$$2b\ddot{b} + \dot{b}^2 = \Lambda_b b^2 - k_b - 2\kappa\dot{a} - b^2 p_b, \tag{16}$$

$$a\dot{a}^2 + b\dot{b}^2 = \frac{\Lambda_a}{3}a^3 - k_a a + \frac{a^3}{3}\rho_a + \frac{\Lambda_b}{3}b^3 - k_b b + \frac{b^3}{3}\rho_b, \tag{17}$$

where p and ρ are the pressure and energy density of the fluid (in $M_{\rm Pl} = (8\pi G)^{-1/2}$ units), respectively, and index a, b denotes the patch where they are defined.

A comment is in order here. While the pressure terms in (15) and (16) trivially satisfy the hypothesis of local matter content, modifications of the constraint equation—the term $a^3\rho_a + b^3\rho_b$ in (17)—do not have a unique form. The most general term modifying (17) must be a function $\rho^{(ab)}$ which satisfies also the separability condition $\rho^{(ab)} = \rho^{(a)} + \rho^{(b)}$, since the constraint in the present model turns out to be the addition of the usual ones on each patch. Indeed, for the FLRW metric with scale factor a, the constraint reads $\mathcal{C}_a = a\dot{a}^2 - \frac{\Lambda_a}{3}a^3 + k_a a - \frac{a^3}{3}\rho_a = 0$, while for the present two-metric model, the constraint reads $\mathcal{C}_a + \mathcal{C}_b = 0$.

The previous characteristic is a consequence of the fact that there is only one time for both patches (and then only one lapse function N) ensuring the time reparametrization invariance. Then, our choice of energy density term respects the separability condition and it reproduces also the standard cosmological scenario if both patches are not connected, that is, $\kappa = 0$.

The conservation law is obtained by taking the time derivative of the constraint and replacing the second derivatives of the scale factors from (15) and (16). For a general energy-density term $\rho^{(ab)}$ the continuity equation reads[4]

$$\dot{\rho}^{(ab)} + \dot{a}a^2 p_a + \dot{b}b^2 p_b = 0. \tag{18}$$

Once we specify the function $\rho^{(ab)}$ to our choice in (17), the previous equation turns out to be

$$a^3[\dot{\rho}_a + 3H_a^2(\rho_a + p_a)] + b^3[\dot{\rho}_b + 3H_b^2(\rho_b + p_b)] = 0, \tag{19}$$

with $H_a = \dot{a}/a$ and $H_b = \dot{b}/b$ the Hubble parameters on each patch.

To summarize, in the present approach where matter on patches a and b are characterized by their pressure and energy density (on each patch), the evolution of the scale factors are given by equations (15) to (17) from which the conservation equation (19) follows.

[4]This is a notation abuse since $\rho^{(ab)}$ does not have the dimensions of energy density.

IV. BAROTROPIC MATTER IN THE EARLY UNIVERSE

We will analyze the effects of the matter presence for the case in which fluids on a and b satisfy the barotropic condition

$$p_a = \omega_a\rho_a, \qquad p_b = \omega_b\rho_b. \tag{20}$$

In the forthcoming analysis, the contributions from cosmological constant will be neglected since we are interested in the early stage of the evolution of the universe, which is an interesting scenario for different physical phenomena like dark matter production [38,40–42] or gravitational waves [48], among others. Also, we set $k_a = 0 = k_b$, the favored scenario consistent with cosmological data [9]. Note also that, in spite of the choice $\Lambda_a = 0 = \Lambda_b$, a sort of cosmological constant term is always present due to the effects of a nonzero value of κ [16]. The equations of evolution, with previous choices, turn out to be

$$2\frac{\ddot{a}}{a} + H_a^2 + \omega_a\rho_a = 2\kappa\frac{\dot{b}}{a^2}, \tag{21}$$

$$2\frac{\ddot{b}}{b} + H_b^2 + \omega_b\rho_b = -2\kappa\frac{\dot{a}}{b^2}, \tag{22}$$

$$a^3\left[H_a^2 - \frac{1}{3}\rho_a\right] + b^3\left[H_b^2 - \frac{1}{3}\rho_b\right] = 0, \tag{23}$$

while the continuity equation reads

$$a^3[\dot{\rho}_a + 3\rho_a H_a^2(\omega_a + 1)] + b^3[\dot{\rho}_b + 3\rho_b H_b^2(\omega_b + 1)] = 0. \tag{24}$$

In the present model, we will look for solutions of (23), respecting the separability hypothesis, and then we look for solutions which are also the solutions of

$$H_a^2 - \frac{\rho_a}{3} = 0, \tag{25}$$

$$H_b^2 - \frac{\rho_b}{3} = 0. \tag{26}$$

The time derivative of previous equations give rise to the following conditions:

$$a^3(\dot{\rho}_a + 3H_a(\omega_a + 1)\rho_a) = 6\kappa\dot{a}\dot{b}, \tag{27}$$

$$b^3(\dot{\rho}_b + 3H_b(\omega_b + 1)\rho_b) = -6\kappa\dot{a}\dot{b}, \tag{28}$$

which, when added, turn out to be (24).

Comparing (27) and (28) with (11) and (12) for the case of NSC, we observe the similar source-sink behavior due to the κ term in the two-metric model. However, the decaying

constant Γ is now time dependent. Moreover, one can rewrite (27) and (28) as

$$\dot{\rho}_a + 3H_a(\omega_a + 1)\rho_a = \Gamma_a \rho_b, \tag{29}$$

$$\dot{\rho}_b + 3H_b(\omega_b + 1)\rho_b = -\Gamma_b \rho_b, \tag{30}$$

with

$$\Gamma_a = 2\kappa \frac{b}{a^2}\delta^{-1/2}, \qquad \Gamma_b = 2\kappa \frac{a}{b^2}\delta^{-1/2}, \tag{31}$$

and $\delta = \rho_b/\rho_a$. The decay functions Γ satisfy $a^3\Gamma_a - b^3\Gamma_b = 0$. In this sense, the two-metric model with matter can be understood as an extension of NSC.

In the following sections we will study the numerical solutions of the set of equations (25) to (28) in two cases. For both scenario the energy density in a patch will have a radiationlike barotropic equation so that we can compare with with NSC (we will refer this content as relativistic), while the patch b contains relativistic matter in one case and nonrelativistic in the other. Even though the numerical solutions found are functions of time, it is convenient to express results in terms of temperatures.

The temperature dependence is incorporated by noticing that in patch a, where relativistic matter dominates, the following relation holds:

$$\rho_a = \frac{\pi^2}{30} g_* T^4, \tag{32}$$

with g_* the number of massless degrees of freedom.

A. Patch b filled with nonrelativistic matter

In this case, as we previously discussed, patch a is filled with relativistic matter while the energy content of b is nonrelativistic. Then we set $\omega_a = 1/3$ and $\omega_b = 0$ and therefore the set of equations (25) to (28) turn out to be

$$\begin{aligned}
\dot{a} &= \sqrt{\frac{\rho_a}{3M_p^2}}a, \\
\dot{b} &= \sqrt{\frac{\rho_b}{3M_p^2}}b, \\
\dot{\rho}_a &= -\frac{4}{\sqrt{3M_p^2}}(\rho_a)^{3/2} + 2\kappa M_p \sqrt{\rho_a \rho_b}\frac{b}{a^2}, \\
\dot{\rho}_b &= -\frac{1}{\sqrt{3M_p^2}}(\rho_b)^{3/2} - 2\kappa M_p \sqrt{\rho_a \rho_b}\frac{a}{b^2},
\end{aligned} \tag{33}$$

where we have restored the Planck mass constant.

Numerical results for the energy density evolution as function of temperature are shown in Figs. 3–5. The quantities of interest, as function of temperature, are $\rho \times (\text{scale factor})^{\ell}$, for some power ℓ.

In all cases with $\kappa \neq 0$ we observe a *drain effect*, namely, the energy density of sector b decreases until it vanishes, while the energy density in a increases. The temperature at which the total drain occurs depends on the value of κ as well as the ratio δ at initial time. This is consistent with the interpretation of source-sink system given by (29).

The dashed line marks the ratio T_{BBN}/T_0 at which the drain of the energy content of b should end. That is the drain must happen, at most, at the temperatures of the order of the temperature of Big Bang Nucleosynthesis (T_{BBN}) or higher than T_{BBN}.

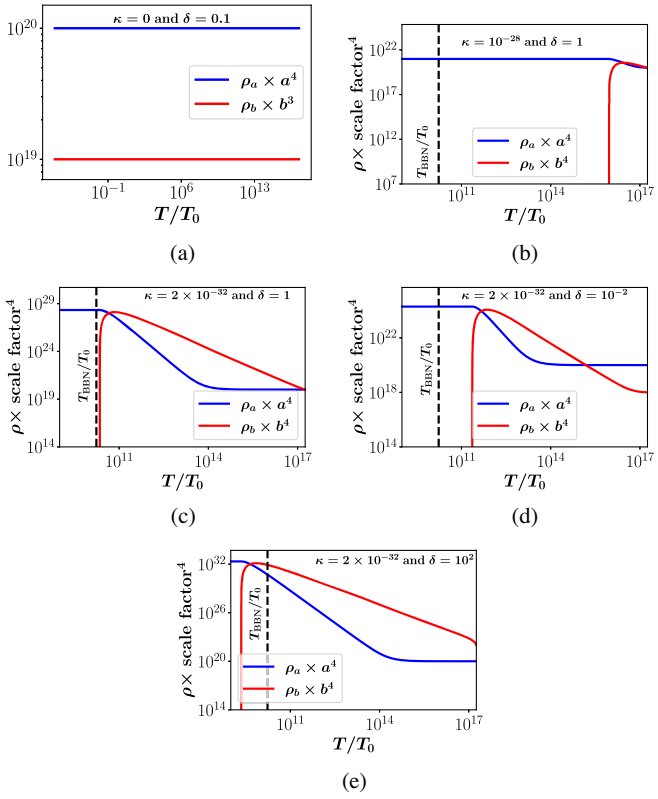

FIG. 3. Evolution of energy density for relativistic matter in a and nonrelativistic matter in b as function of the temperature T/T_0. T_0 is the CMB temperature at present ($T_0 = 2.33 \times 10^{-13}$ GeV). The dashed line indicates the Big Bang Nucleosynthesis temperature at which ρ_b should vanish. For all cases the initial density $\rho_a = 10^{20}$ GeV. Panel (a) shows the case $\kappa = 0$. Panels (b) and (c) are the solutions for $\delta = 1$ and different values of κ. The panels (d) and (e) show the evolution for $\delta \neq 1$ and same value of κ.

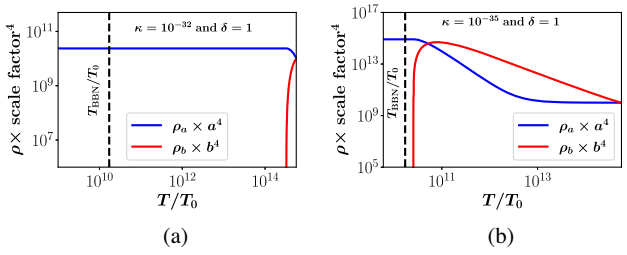

FIG. 4. Evolution of energy density for different values of κ and initial condition $\rho_a = 10^{10}$ GeV with $\delta = 1$.

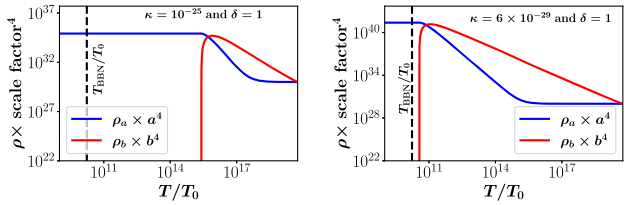

FIG. 5. Evolution of energy density for different values of κ and initial condition $\rho_a = 10^{30}$ GeV with $\delta = 1$.

The panel (a) in Fig. 3 shows the situation for $\kappa = 0$ in order to check that the systems are decoupled in such cases and the energy densities evolve as it is expected for radiation and nonrelativistic matter. That is, $\rho_a \propto a^{-4}$ and $\rho_b \propto b^{-3}$.

Panels (b) and (c) of Fig. 3 show the case of initial ratio $\delta = 1$ and it is possible to observe that the decay of b happens at higher temperatures (compared with $T_{\rm BBN}$) as κ increases. Indeed, it is enough to have $\kappa \gtrsim 10^{-32}$ in order to have a complete decay of energy content of b sector at $T_{\rm BBN}$. This is consistent with the fact that Γ_a in (29) is proportional to κ.

Let us take now the value of κ so that the total drain occurs at the desired temperature for a symmetric initial density condition ($\delta = 1$), situation shown in panel (c). The effect of initial condition $\delta > 1$ and $\delta < 1$ can be observed in panels (d) and (e) in the same figure. We observe in panel (e) that when b patch has more energy to drain (compared with the energy of a patch) at the initial time, the complete process takes a longer time, so that the total decay of energy in patch b happens at temperatures smaller than $T_{\rm BBN}$, which is an unfavorable scenario.

In all previous cases the initial value of energy density in a is $\rho_a = 10^{20}$ GeV. The effect of a different initial condition for ρ_a has been also addressed and the results are shown in Figs. 4 and 5. In the first, the initial value of energy density is $\rho_a = 10^{10}$ GeV while it is $\rho_a = 10^{30}$ GeV in the second. For both cases we have chosen $\delta = 1$. We conclude that the value of κ for which the total drain happens at the desired temperature $T_{\rm BBN}$ decreases as the initial density ρ_a decreases, which is consistent with our previous result in Fig. 3, panels (b) and (c).

To summarize, the temperature at which the energy density of sector b vanishes, producing an increment of the energy content in sector a (a source-sink effect) depends on the values of κ, the initial value of the energy density in sector a,[5] and δ. Large values of κ produce a fast decay of ρ_b while large values of initial ρ_a slow down the decay rate. For a fixed κ, instead, large values of initial ρ_b also slow down the decay rate.

[5]Naturally, it depends on the initial value of ρ_b through δ.

In the following section we will analyze the case in which the sector b has relativistic matter also and we will show that previous conclusions are also valid for such a case.

B. Patch b filled with relativistic matter

In this case, the patches a and b contain relativistic matter ($\omega_a = \omega_b = 1/3$). The set of equations (25) to (28) to determine time evolution of scale factors and the energy density (with the Planck mass restored) are

$$\begin{aligned}
\dot{a} &= \sqrt{\frac{\rho_a}{3M_p^2}}a, \\
\dot{b} &= \sqrt{\frac{\rho_b}{3M_p^2}}b, \\
\dot{\rho}_a &= -\frac{4}{\sqrt{3M_p^2}}(\rho_a)^{3/2} + 2\kappa M_p\sqrt{\rho_a\rho_b}\,\frac{b}{a^2}, \\
\dot{\rho}_b &= -\frac{4}{\sqrt{3M_p^2}}(\rho_b)^{3/2} - 2\kappa M_p\sqrt{\rho_a\rho_b}\,\frac{a}{b^2}.
\end{aligned} \tag{34}$$

The evolution of energy densities as functions of temperatures is shown in Figs. 6–8 for different values of initial ρ_a and $\delta = 1$.

We observe for all cases how the energy density of relativistic matter in sector a increases at expenses of the energy content of sector b until the energy on this sector is completely drained. For the initial condition $\rho_a = 10^{10}$ GeV we can compare the relativistic–relativistic case depicted in Fig. 6 with the relativistic–nonrelativistic case in Fig. 4. Again, for large values of κ, the total drain occurs for temperatures greater than the BBN temperature. The value of κ at which the total drain happens near $T_{\rm BBN}$ is slightly smaller compared with the radiation-matter case.

The effects of a larger initial value of ρ_a (with $\delta = 1$) are shown in Figs. 7 and 8 which should be compared with Figs. 3 [panels (b) and (c)] and 5, respectively. The general features previously discussed are observed here and, additionally, a small value of κ, compared with the relativistic–nonrelativistic case, is necessary in order to reach the total drain at $T_{\rm BBN}$. In other words, for a fixed

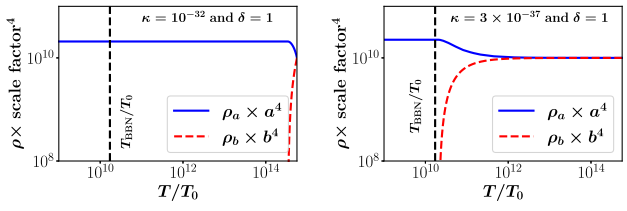

FIG. 6. Evolution of radiation content in patches a and b as function of the temperature. Panels (a) and (b) show the energy densities evolution for an initial condition $\rho_a = 10^{10}$ GeV and $\delta = 1$ and different values of κ.

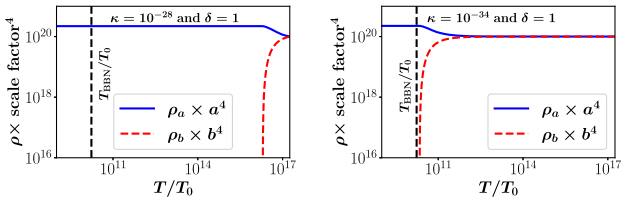

FIG. 7. Evolution of radiation content in patches a and b as function of the temperature. In the y axes we have plotted $\rho_a \times a^4$ and $\rho_b \times b^4$. Panels (a) and (b) show the energy densities evolution for an initial condition $\rho_a = 10^{20}$ GeV and $\delta = 1$ and different values of κ.

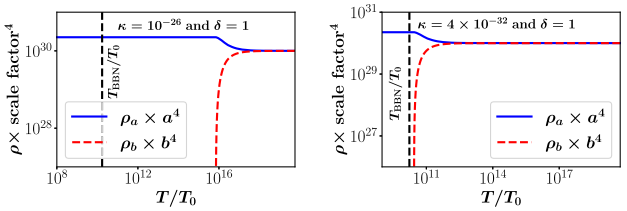

FIG. 8. Radiation content in patches a and b as function of the temperature. Panels (a) and (b) show the energy densities evolution for an initial condition $\rho_a = 10^{30}$ GeV and $\delta = 1$.

value of κ and initial $\delta = 1$, the drain of energy from b to a happens faster if b contains radiation compared with the case in which b contains nonrelativistic matter.

V. DISCUSSION AND CONCLUSIONS

In this work we have presented an extension of a cosmological model with two scale factors in order to include matter. The two scale factors might represent two sectors of a universe (two patches) [49], or even two different universes in a multiverse scenario [50] which are causally connected only through a deformation of the Poisson bracket structure. In this sense, this model is a sort of a noncommutative cosmology. The model is analogous of the Landau problem in the space of metrics [17].

The evolution of matter in such universe has been addressed, and, in order to do that, we have assumed a) the matter content on each patch do not interact—our matter-independent hypothesis—and b) the modification of equations of motion is minimal and it reduces to the usual equations of motion of General Relativity when the deformation parameter $\kappa = 0$.

Under such hypotheses, the equations of the evolution of the energy density have been solved numerically for two cases. In both, one of the patches contains relativistic matter while the content of the other is relativistic in one case and nonrelativistic in the second one.

The cases analyzed show an energy transfer from patch b to patch a in a sort of source-sink effect. The energy content of b drains completely to a at some temperature $T_{\rm drain}$ which can be chosen to be equal to $T_{\rm BBN}$ in order to restrict the possible values of the deformation parameter κ. Note that the process is not symmetric under the change $a \leftrightarrow b$, since equations of motion do not have this symmetry. The system is symmetric under the previous change of scale factors and $\kappa \to -\kappa$.

This source-sink effect is also present in the context of string theory formulated in a generalized noncommutative space [51–53] in the low energy limit. There, the effective action has contributions from both sectors of the doubled phase space, and dark matter and dark energy arise as matter degrees of freedom and the curvature of the dual space, respectively.

The rate at which the drain occurs [the function Γ defined in (31)] depends on time through the scale factors and δ, and it depends linearly on the deformation parameter κ. In spite of this time (temperature) dependence, it is always possible to choose κ so that the total drain happens at the desired temperature $T_{\rm BBN}$ and this value of κ will depend on the initial energy content of a and b.

It is instructive to compare the behavior of the functions Γ^{-1} [with dimensions of $(\text{time})^{-1}$] for the radiation-radiation and radiation-matter cases. In Fig. 9—where blue lines correspond to the radiation-matter (Sec. IV A) and red lines to radiation-radiation (Sec. IV B)—this behavior is shown. Here Γ_a^{-1} appears in a solid line while a dashed line is Γ_b^{-1}.

For fixed value of κ and initial $\delta = 1$, we observe that radiation decays faster than matter in patch b, or, in other words, the energy drain of relativistic matter happens faster than the nonrelativistic one.

Previous effect suggests that the present model can be understood as a different type of nonstandard cosmology and it also suggests to include dark matter in one of the patches. This analysis will be presented in forthcoming works.

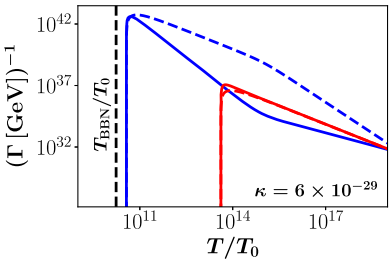

FIG. 9. Evolution of Γ^{-1} in terms of the temperature. Solid lines represent Γ_a and the dashed lines Γ_b. In blue appears the radiation-matter case (Sec. IV A) while the radiation-radiation (Sec. IV B) is shown in red. It can be observed that for the same value of κ the decay of radiation from b to a is faster than the case of matter.

ACKNOWLEDGMENTS

This work was supported by Dicyt-USACH Grants No. USA1956-Dicyt (C. M.) and No. Dicyt-041931MF (F. M.).

[1] S. Weinberg, *Cosmology* (Oxford University Press, New York, 2008).
[2] E. W. Kolb and M. S. Turner, *The Early Universe* (Taylor and Francis Group, Boca Ratón, FL, 1990), Vol. 69.
[3] F. Zwicky, Helv. Phys. Acta **6**, 110 (1933).
[4] K. C. Freeman, Astrophys. J. **160**, 811 (1970).
[5] G. Bertone and D. Hooper, Rev. Mod. Phys. **90**, 045002 (2018).
[6] P. Salucci, Found. Phys. **48**, 1517 (2018).
[7] A. G. Riess, A. V. Filippenko, P. Challis, A. Clocchiatti, A. Diercks, P. M. Garnavich, R. L. Gilliland, C. J. Hogan, S. Jha, R. P. Kirshner *et al.*, Astron. J. **116**, 1009 (1998).
[8] S. Perlmutter, G. Aldering, G. Goldhaber, R. A. Knop, P. Nugent, P. G. Castro, S. Deustua, S. Fabbro, A. Goobar, D. E. Groom *et al.*, Astron. J. **517**, 565 (1999).
[9] P. Zyla *et al.* (Particle Data Group), Prog. Theor. Exp. Phys. **2020**, 083C01 (2020).
[10] A. Vilenkin, Phys. Rep. **121**, 263 (1985).
[11] P. Sikivie, Phys. Rev. Lett. **48**, 1156 (1982).
[12] A. Lukas, B. A. Ovrut, K. S. Stelle, and D. Waldram, Phys. Rev. D **59**, 086001 (1999).
[13] E. Flanagan, S.-H. Tye, and I. Wasserman, Phys. Rev. D **62**, 024011 (2000).
[14] P. Peebles and A. Vilenkin, Phys. Rev. D **59**, 063505 (1999).
[15] A. D. Linde, *Particle Physics and Inflationary Cosmology* (CRC Press, Boca Raton, London, New York, 1990), Vol. 5.
[16] H. Falomir, J. Gamboa, F. Méndez, and P. Gondolo, Phys. Rev. D **96**, 083534 (2017).
[17] H. Falomir, J. Gamboa, P. Gondolo, and F. Méndez, Phys. Lett. B **785**, 399 (2018).
[18] H. Falomir, J. Gamboa, and F. Mendez, Symmetry **12**, 435 (2020).
[19] D. G. Boulware and S. Deser, Phys. Rev. D **6**, 3368 (1972).
[20] V. Baccetti, P. Martin-Moruno, and M. Visser, Classical Quantum Gravity **30**, 015004 (2013).
[21] C. de Rham and G. Gabadadze, Phys. Rev. D **82**, 044020 (2010).
[22] C. de Rham, G. Gabadadze, and A. J. Tolley, Phys. Rev. Lett. **106**, 231101 (2011).
[23] S. F. Hassan and R. A. Rosen, Phys. Rev. Lett. **108**, 041101 (2012).
[24] S. F. Hassan and R. A. Rosen, J. High Energy Phys. 02 (2012) 126.
[25] F. Bayen, M. Flato, C. Fronsdal, A. Lichnerowicz, and D. Sternheimer, Ann. Phys. (N.Y.) **111**, 61 (1978).
[26] B. V. Fedosov, J. Diff. Geom. **40**, 213 (1994).
[27] M. Kontsevich, Lett. Math. Phys. **66**, 157 (2003).
[28] A. S. Cattaneo and D. Indelicato, Lond. Math. Soc. Lect. Note Ser. **323**, 79 (2004), https://www.zora.uzh.ch/id/eprint/21691/.
[29] L. Freidel, R. G. Leigh, and D. Minic, J. High Energy Phys. 09 (2017) 060.
[30] L. Freidel, R. G. Leigh, and D. Minic, Phys. Rev. D **96**, 066003 (2017).
[31] L. Freidel, J. Kowalski-Glikman, R. G. Leigh, and D. Minic, Phys. Rev. D **99**, 066011 (2019).
[32] L. Freidel, R. G. Leigh, and D. Minic, Int. J. Mod. Phys. D **24**, 1544028 (2015).
[33] L. Freidel, R. G. Leigh, and D. Minic, J. Phys. Conf. Ser. **804**, 012032 (2017).
[34] L. Freidel, R. G. Leigh, and D. Minic, Int. J. Mod. Phys. A **34**, 1941004 (2019).
[35] P. Berglund, T. Hübsch, and D. Minic, Lett. High Energy Phys. **2021**, 186 (2021).
[36] R. J. Scherrer and M. S. Turner, Phys. Rev. D **31**, 681 (1985).
[37] S. Hamdan and J. Unwin, Mod. Phys. Lett. A **33**, 1850181 (2018).
[38] G. F. Giudice, E. W. Kolb, and A. Riotto, Phys. Rev. D **64**, 023508 (2001).
[39] G. Gelmini and P. Gondolo, Phys. Rev. D **74**, 023510 (2006).
[40] C. Maldonado and J. Unwin, J. Cosmol. Astropart. Phys. 06 (2019) 37.
[41] P. Arias, N. Bernal, A. Herrera, and C. Maldonado, J. Cosmol. Astropart. Phys. 10 (2019) 47.
[42] N. Bernal, F. Elahi, C. Maldonado, and J. Unwin, J. Cosmol. Astropart. Phys. 11 (2019) 26.
[43] L. Visinelli, Symmetry **10**, 546 (2018).
[44] D. J. H. Chung, E. W. Kolb, and A. Riotto, Phys. Rev. D **60**, 063504 (1999).
[45] E. W. Kolb, A. Notari, and A. Riotto, Phys. Rev. D **68**, 123505 (2003).
[46] M. Kawasaki, K. Kohri, and N. Sugiyama, Phys. Rev. D **62**, 023506 (2000).
[47] S. Hannestad, Phys. Rev. D **70**, 043506 (2004).
[48] N. Bernal, A. Ghoshal, F. Hajkarimc, and G. Lambiase, J. Cosmol. Astropart. Phys. 11 (2020) 051.
[49] S. Rasouli, J. Marto, and P. Moniz, Phys. Dark Universe **24**, 100269 (2019).
[50] A. Linde, Rep. Prog. Phys. **80**, 022001 (2017).
[51] P. Berglund, T. Hubsch, and D. Minic, Int. J. Mod. Phys. D **28**, 1944018 (2019).
[52] L. Freidel, J. Kowalski-Glikman, R. G. Leigh, and D. Minic, arXiv:2104.00802.
[53] P. Berglund, T. Hübsch, and D. Minić, Phys. Lett. B **798**, 134950 (2019).